J. Environ. Nanotechnol.
Volume 5, No.2(2016) pp.11-16
ISSN (Print): 2279-0748
ISSN (Online): 2319-5541
doi:10.13074/jent.2016.06.162189

Synthesis, Structural and Antibacterial Properties of Mg Doped ZnO Nanoparticles

A. Jafar Ahamed[1*], P. Vijaya Kumar[2], M. Karthikeyan[3]

[*1,2,3]Department of Chemistry, Jamal Mohamed Tamil Nadu College (Autonomous), Tiruchirappalli, TN, India.

Received: 18.02.2016 *Accepted: 23.04.2016*

Abstract

Zinc oxide (ZnO) nanoparticles were chemically synthesized with magnesium doping and characterized through UV–visible spectroscopy, X-ray diffraction (XRD), high resolution transmission electron microscopy (HRTEM), energy dispersive X-ray (EDAX) techniques and photoluminescence (PL) spectroscopy. Magnesium doped ZnO nanoparticles were found to be crystalline having a single phase as confirmed by XRD and HRTEM. The antibacterial activity of Mg doped ZnO nanoparticles synthesized by a simple co-precipitation technique have been investigated against Escherichia coli and Staphylococcus aureus bacterial strains. It has been interestingly observed that Mg doping has enhanced the inhibitory activity of ZnO against S. aureus more efficiently than the E. coli bacterial strain.

Keywords: *Antibacterial activity; E. coli; Mg doped ZnO; Nanoparticles; S. aureus.*

1. INTRODUCTION

Zinc oxide is a wide band gap semiconductor with a direct band gap of 3.37 eV and large excitonic binding energy (60 meV) (Janotti *et al.* 2009). Nanostructured zinc oxide has shown a great potential for applicationsin UV laser devices (Dai *et al.* 2003), quantum wells with superior interface morphologies (Beaur *et al.* 2011), cell imaging (Xiong *et al.* 2008) and solar cells (Kruefu *et al.* 2010). Recently, it has been reported that the doping of ZnO nanostructures with other elements can enhance its various properties. Commonly, different elements as a dopant in ZnO can be categorized into two groups: one group can substitute for zinc (Zn) and the second group for oxygen (O). These different dopants can tune various properties of ZnO nanostructures (Jung *et al.* 2011).

There have been many methods for the synthesisof ZnO nano particles and also for doping. For thesynthesis of ZnO nanoparticles, mostly reportedmethods are from sol–gel (Omri *et al.* 2014), co-precipitation (Raoufi *et al.* 2013), hydrothermal (Kumar *et al.* 2012), solvothermal (Chen *et al.* 2015), mechanochemical (Radzimska *et al.* 2014), spray pyrolysis (Ghaffarian *et al.* 2011) etc. Among these methods, precipitation method is a bestmethod and also cost effective. The process can becontrolled easily. In this work, Mg was used as dopantto ZnO and their structural, optical, antibacterial properties are analysed.

2. EXPERIMENTAL METHOD

Mg doped ZnO nanoparticles were synthesized byco-precipitation method. Zinc nitrate hexahydrate (Sigma Aldrich), Sodium hydroxide (Sigma Aldrich) and Magnesium nitrate hexahydrate (Sigma Aldrich), were AR grade and used in the synthesis of Mg-doped Zinc Oxide without further purification. For synthesis of Mg doped ZnO nanoparticles, 0.005 M of aqueous Magnesium nitrate hexahydrate solution was added into 0.095 M of aquous zinc nitrate solution. 0.8 M of aquous NaOH solution was added drop by drop to homogenous mixture to get a white precipitate. The solution with the white precipitate was stirred at room temperature and then temperature of 60 °C for 4 hr. This solution was refluxed at room temperature for 24 hr. Then, a clear solution was obtained, which found to be stabe at a ambient condition. Thereafter, the solution was washed several times with double distilled water and ethanol. Finally, the precipitate was dried at 120 °C. Thus Mg doped ZnO nanopowder was obtained. These samples were annealed at 500 °C for 6 hr.

A. Jafar Ahamed** **Tel. no: +919003576896
Email: agjafar@yahoo.co.in

2.1 Antimicrobial activity of ZnO NPs

Antimicrobial activity of Mg doped ZnO nanoparticles were done by agar well diffusion method against two pathogenic bacterial strains *S.aureus* (gram positive) and *E. coli* (gram negative) on Muller-Hinton agar, according to the Clinical and Laboratory Standards Institute (CLSI) (Wright *et al.* 2000). The media plates (MHA) were streaked with bacteria 2-3 times by rotating the plate at 60 °C angles for each streak to ensure the homogeneous distribution of the inoculums. Then the agar plates were swabbed with 100 mL each of overnight cultures of *S.aureus* and *E. coli* using a sterile L-shaped glass rod. Using a sterile cork-borer, wells (6 mm) were created in each petri plate. Varied concentrations of ZnO NPs (1 mg/ml, 3 mg/ml and 5 mg/ml for both G+ and G- both bacteria) were loaded onto the petri plates followed by incubation for 24 hr at 37 °C, for bacteria. After the incubation period, the diameter of the zone of inhibition (DZI) was recorded. Kanamycin (Hi-Media) was used as the positive control against gram negative and gram positive bacteria respectively to compare the efficacy of the test samples.

2.2 Characterization techniques

The Mg doped ZnO NPs were characterized by X-ray diffractometer (model: X'PERT PRO PANanalytical). The diffraction pattern was recorded in the range of 25°-80° for the ZnO NPs samples where the monochromatic wavelength of 1.54 Å used. The morphology of the synthesized Mg doped ZnO NPs was examined using HRTEM. Sample for HRTEM analysis was prepared by drop coating the nanoparticles solutions on carbon-coated copper grids at room temperature. The excess nanoparticles solutions were removed with filter paper. The copper grid was finally dried at room temperature and was subjected to TEM analysis by the instrument Tecnai F20 model operated at an accelerating voltage of 200 kV. The samples were analyzed by EDAX (model: ULTRA 55). The FT-IR spectrum was recorded in the range of 400-4000 cm^{-1} by using Perkin-Elmer spectrometer.

3. RESULTS AND DISCUSSION

3.1 Structural studies of Mg doped ZnO nanoparticles

Fig. 1 shows the XRD pattern of the as synthesized Mg^{2+} doped ZnO nanoparticles. The XRD peaks are appeared at angles (2θ) of 31.702˚, 34.364˚, 36.188˚ and 74.25˚ corresponding to (100), (002) and (101) planes of ZnO nanoparticles. Similarly, other peaks found at angles (2θ) of 47.490, 56.532, 62.816, 67.90, 69.15, 72.52 and 76.88 are corresponding to (102), (110), (103), (112), (201), (004) and (202) planes of ZnO NPS. The standard diffraction peaks show that the hexagonal wurtzite structure of ZnO NPs with space group of p63mc. It is also confirmed by the JCPDS data (card No: 361451). It is also observed that there is no impurity phase found in the Mg^{2+} doped ZnO sample, because of ionic radii of Mg (0.66 Å). The average crystallite size of the Mg^{2+} doped ZnO NPs was estimated from X-ray line broadening of the diffraction peaks using Debye Scherrer's relation.

$$\text{Average crystallite size (D)} = \frac{0.9\,\lambda}{\beta \cos\theta} \qquad (1)$$

Where, λ is the wave length of X-ray used (1.54060 Å), β is the angular peak width at half maximum in radians and θ is Bragg's diffraction angle. The average crystallite size is calculated as 42 nm for Mg^{2+}doped ZnO NPs.

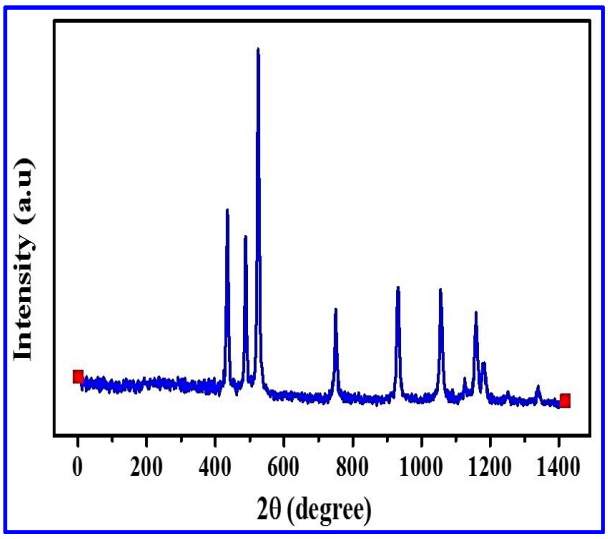

Fig. 1: XRD pattern of Mg doped ZnO nanoparticles

3.2 Morphological studies of Mg^{2+} doped ZnO nanoparticles

The HRTEM images of the Mg^{2+} doped ZnO nanoparticles are shown in fig. 2a and 2b. From the figures we can find that the Mg^{2+} doped ZnO nanoparticles form a fish like structure. The average thickness of the particles is found to be 45 nm. The thickness is due to the distortion in the host material incorporated with Mg^{2+}. The alkaline metal ions decrease the nucleation and subsequent growth rate of ZnO nanoparticles, so that the nanoparticles thickness is reduced. The crystalinity of the synthesized Mg^{2+} doped ZnO nanoparticle was examined by selected area diffraction studies. Fig. 2c shows the fish like structure with regular spacing of clear lattice planes.

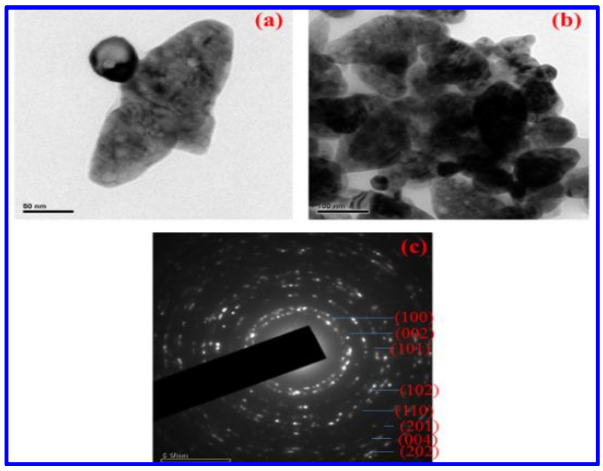

Fig. 2a & 2b: HRTEM images & Fig. 2c: SAED studies of Mg^{2+} doped ZnO nanoparticles

3.3 Energy dispersive analysis X-ray (EDAX) studies

The compositional analysis of the Mg^{2+} doped ZnO NPs are carried out by using EDAX analysis. The typical EDAX spectrum of the alkaline metal ion (Mg^{2+}) doped ZnO NPs are recorded in fig. 3. From the EDAX analysis, the amounts of metals present in the Mg doped ZnO NPs are Zn = 63.68%, Mg = 1.04% and O = 16.76%. It is evident that, the expected elements are present in the synthesized samples.

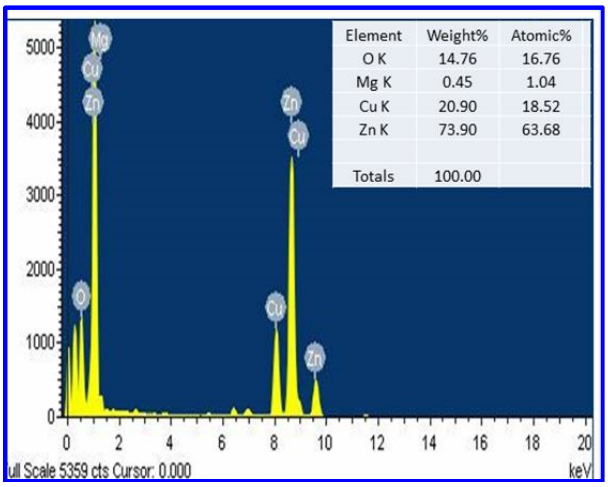

Fig. 3: EDAX spectrum of Mg^{2+} doped ZnO nanoparticles

3.4 UV-visible studies of Mg^{2+} doped ZnO nanoparticles

The optical properties of Mg^{2+}doped ZnO NPs are characterized by UV-vis spectrumas shown in fig. 4. From the absorption spectra, the absorption peaks are found at 391 nm for pure ZnO NPs whereas the peaks are observed at 388 nm for Mg doped ZnO NPs, which can be attributed to the photo excitation of electrons from valence band to conduction band.

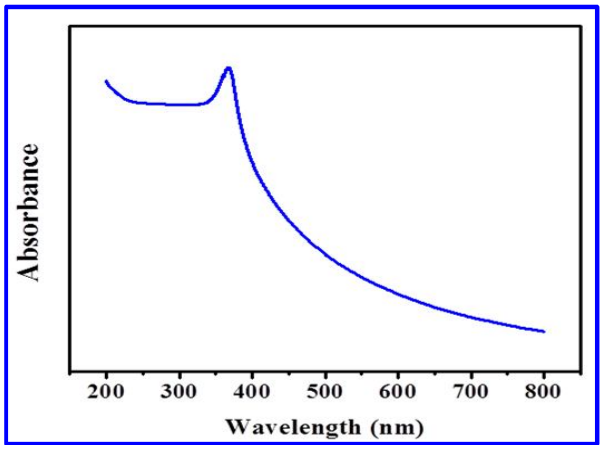

Fig. 4: UV-vis spectrum of Mg2+ doped ZnO nanoparticles

The results also show that theincrease in Mg concentration leads to an increase in transmittance (Liu *et al.* 1992).

3.5 Fourier Transform Infra-Red (FT-IR) Spectroscopic Analysis

FT-IR spectroscopic analysis reveals the vibrational frequencies of the alkaline metal ion (Mg^{2+}) doped ZnO NPs. The recorded FT-IR spectra are shown in fig. 5. A peak in the range of 3020-3650 cm^{-1} corresponds to the vibrational mode of O-H bond (Zandi *et al.* 2011). The symmetric C=O bands are observed at 1442 cm^{-1} for the pure ZnO samples. The band at 1435cm^{-1} is attributed to Mg-O stretching vibration (Munoz Hernandez *et al.* 2009). In the present investigation, Mg doped ZnO shows the stretching vibration at 1436 cm^{-1}.

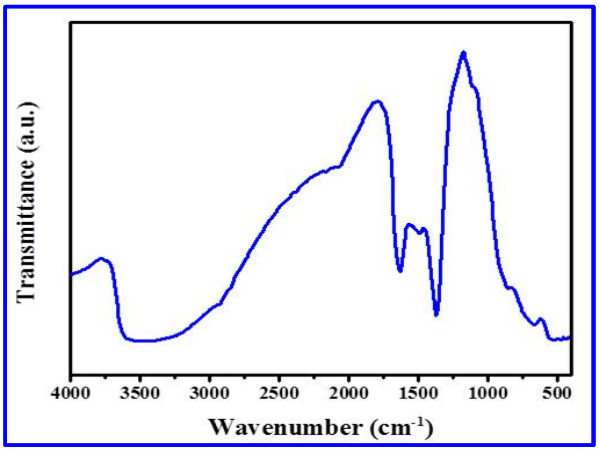

Fig. 5: FTIR spectrum of Mg^{2+} doped ZnO nanoparticles

3.6 Photoluminescence studies

The photoluminescence spectra of the as-synthesized Mg^{2+}doped ZnO NPs sample is recorded with the excited wavelength of 325 nm are shown in fig. 6. The PL emission is observed for the synthesized sample covering from the very short wavelength of 388 nm to long wavelength of 524 nm, which is in accordance with results in the literature (Singh *et al.* 2012; Malkaj *et al.* 2007; Fan *et al.* 2005). A relatively sharp, weak UV emission band at 3.25eV (388 nm) and a broad stronger emission band in the green partof the visible spectrum with a maximum intensity at 2.6eV (524 nm) are observed. The UV band is due to the radiative annihilation of excitons (exciton emission). The origin ofthe broad green emission band at 2.38 eV is attributed to surface anion vacancies (Malkaj *et al.* 2007). It involves the tunnelling of surface-bound electrons through pre-existing trapped holes. Surface state is regarded as a main factor that determines visible luminescence of ZnO due to its defects or vacancies which are mainly located on the surface of NPs. The ZnO NPs are highly crystallized, i.e., there are almost no amorphous phases on the ZnO surface.

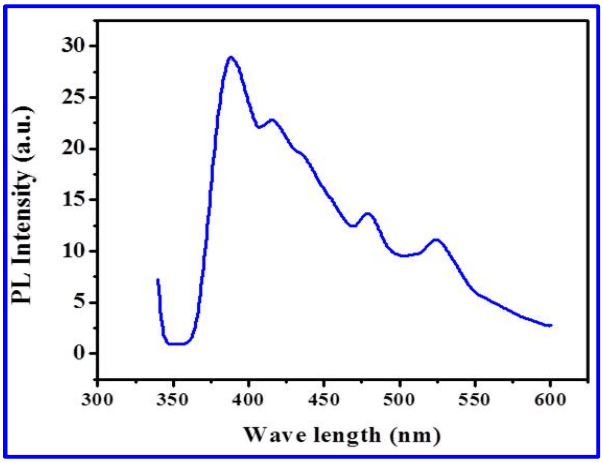

Fig. 6: Photoluminescence spectrum of Mg^{2+} doped ZnO nanoparticles

3.7 Antibacterial activity

In the present scenario, the NPs are studied extensively to explore their utility as a potential antibacterial agent. Several factors such as less toxicity and heat resistance are accountable forthe use of NPs in the biological applications (Prasad *et al.* 2010; Brayner *et al.* 2006).

In the current study, Mg^{2+} doped ZnO NPs are tested against gram negative (*Escherichia coli*) and gram-positive bacteria (*Staphylococcus aureus*) using disc diffusion method to determine their ability as a potential antimicrobial agent. They clearly indicate that the Mg^{2+} doped zinc oxide nanoparticles inhibit the growth of both gram-negative and positive bacteria and the zone of inhibition increases with the increase in concentration of nanoparticles which are shown in table 1.

Table 1. Zone of inhibition of Mg^{2+} doped ZnO nanoparticles against bacterial strains

S. No	Conc. of Mg^{2+} doped ZnO nanoparticles (µL)	Zone of inhibition (mm)	
		Gram positive strains	Gram negative strains
		S. aureus	*E. coli*
1	1	13.5	11
2	3	15.0	12
3	5	16.0	14

It is clear from table 1, that Mg^{2+} doped zinc oxide nanoparticles have shown almost similar antibacterial activities against all the pathogens. The variation in the sensitivity or resistance to both gram-positive and gram-negative bacteria populations could be due to the differences in the cell structure, physiology, metabolism or degree of contact of organisms with nanoparticles.

The antibacterial efficiency of ZnO NPs generally depends on the higher ROS which is mainly attributed to the larger surface area, increase in oxygen vacancies, the diffusion ability of the reactant molecules and the release of Zn^{2+} (Brayner *et al.* 2011). The superoxide radical, hydroxyl radical and hydrogen peroxide belonged to ROS group can cause damage to DNA, cellular protein and may even lead to cell death (Becker *et al.* 2011). Generally, nanoparticles with better photo catalytic activity have larger specific surface area and smaller crystal size that increase oxygen vacancies yielding to higher ROS (Brayner *et al.* 2006). In addition, crystal growth direction is another important factor for generation of ROS. Earlier studies have proved that the terminal polar face (001) is more active than the nonpolar surface (00-1) for photocatalytic H_2O_2 generation (Applerot *et al.* 2009). Similarly, Zn polar terminal has exhibited strong UV luminescence rather than On polar terminal (Jang *et al.* 2006). Fig. 7 shows the zone of inhibition formed around each disc loaded with test samples indicating the antibacterial activity.

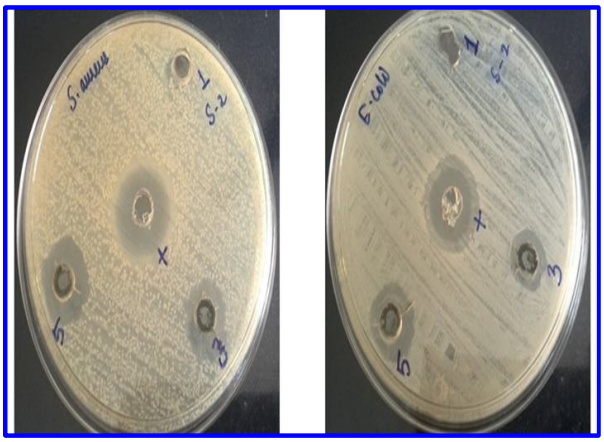

Fig. 7: Zone of inhibition of Mg doped ZnO nanoparticles against *S. aureus* and *E. coli*

4. CONCLUSION

Chemical synthesis of Mg-doped ZnO nanoparticles was successfully achieved with crystalline and wurtzite like structure. From the HRTEM images, the particles were found to have nano fish like morphology. From the EDAX analysis, the chemical compositions were estimated for the prepared samples. Using the recorded FT-IR spectra, the various vibrational frequencies were assigned for the Mg doped ZnO samples. Photoluminescence studies showed that doping materials altered the band emission, which is due to zinc vacancy, oxygen vacancy and surface defects. The antibacterial studies performed against a set of bacterial strains showed that the Mg doped ZnO NPs possessed more antibacterial property. The antibacterial property of the ZnO samples was found mainly due to the combination of reactive oxygen species and the release of Zn^{2+}. The effect was not originated from the release of Mg^{2+} because any peak (impurity phase) corresponding to Mg was not observed from the XRD pattern of the Mg doped ZnO NPs.

REFERENCES

Applerot, G., Lipovsky, A., Dror, R., Perkas, N., Nitzan, Y., Lubart, R. and Gedanken, A., Enhanced antibacterial of nanocrystalline ZnO due to increased ROS-mediated cell injury, *Adv. Funct Mater.*,19, 842-852(2009). doi: 10.1002/adfm.200801081

Beaur, L., Bretagnon, T., Gil, B., Kavokin, A., Guillet, T., Brimont, C., Tainoff, D., Teisseire, M. and Chauveau, J. M., Exciton radiative properties in nonpolar homoepitaxial ZnO/ (Zn,Mg) O quantum wells, *Phys. Rev.* B., 84(16), 165312/01-08(2011). doi:10.1103/physrevb.84.165312

Becker, J., Raghupathi, K. R., Pierre, J. S., Zhao, D., Koodali, R. T., Tuning of the crystallite and particle sizes of ZnO nanocrystalline materials in solvothermal synthesis and their photocatalytic activity for dye degradation, *J. Phys. Chem C.*, 115(28), 13844-13850(2011). doi: 10.1021/jp2038653

Brayner, R., Ferrari-lliou, R., Brivois, N., Djediat, S., Benedetti, M. F. and Fievet, F., Toxicological impact studies based on Escherictia coli bacteria in ultrafine ZnO nanoparticles colloidal medium, *Nano Lett.*, 6(4), 866-870(2006). doi: 10.1021/nl052326h

Chen, Y., Zhang, C., Huang, W., Situ, Y. and Huang, H., Multimorphologies nano-ZnO preparing through a simple solvothermal method for photocatalytic application, *Mater Lett.*,141, 294-297(2015). doi:10.1016/j.matlet.2014.11.106

Dai, Z. R., Pan, Z. W. and Wang, Z. L., Novel nanostructures of functional oxides synthesized by thermal evaporation, *Adv. Funct. Mater.*, 13(1), 09-24(2003). doi: 10.1002/adfm.200390013

Fan, X. M., Lian, J. S., Zhao, L. and Liu, Y., Single violet luminescence emitted from ZnO flims obtained by oxidation of Zn film on quartz glass, *Appl. Sur. Sci.*, 252(2), 420-424(2005). doi:10.1016/j.apsusc.2005.01.018

Ghaffarian, H. R., Saiedi, M., Sayyadnejad, M. A. and Rashidi, A. M., Synthesis of ZnO nanoparticles by spray pyrolysis method, *Iran J. Chem. Chem. Engg.*, 30(1), 01-06(2011).

Jang, E. S., Won, J. H., Hwang, S. J. and Choy, J. H., Fine tuning of the face orientation of ZnO crystals to optimize their photocatalytic activity, *Adv. Mater.*, 18(24), 3309-3312(2006). doi: 10.1002/adma.200601455

Janotti, A. and Van de Walle, C. G., Fundamentals of zinc oxide as a semiconductor, *Rep. Prog. Phys.*, 72(12), 126501/01-29(2009). doi:10.1088/0034-4885/72/12/12650

Jung, M., Kim, S. and Ju, S., Enhancement of green emission from Sn-doped ZnO nanowires. *Opt. Mater. (Amst).*, 33(3), 280-283(2011). doi:10.1016/j.optmat.2010.08.029

Kruefu, V., Peterson, E., Khantha, C., Siriwong, C., Phanichphant, S. and Carroll, D. L., Flame-made niobium doped zinc oxide nanoparticles in bulk heterojunctions solar cells, *Appl. Phys. Lett.*, 97, 053302/01-03(2010).

Kumar, S. and Sahare, P. D., Observation of band gap and surface defects of ZnO nanoparticles synthesized via hydrothermal route at different reaction temperature, *Optics. Commun.*, 285, 5210-5216(2012). doi:10.1016/j.optcom.2012.07.125

Liu, M., Kitai, A.H., and Mascher, P., Point defects and luminescence centes in zinc oxide and zinc oxide doped with manganese, *J. Lumin.*, 54(1), 35-42(1992). doi:10.1016/0022-2313(92)90047-D

Malkaj, P., Dalas, E., Kanellopoulou, D. G., Chrissanthopoulos, A. and Sevastos, D., Calcite particles formation in the presence of soluble polyvinyl- alcohol matrix, *Powder Tech*., 177(2), 71-76(2007). doi:10.1016/j.powtec.2007.02.012

Munoz Hernandez, G., Escobedo Morales, A. and Pal, U., Thermolytic growth of ZnO nanocrystals: morphology control and optical poperties, *Cryst. Growth. Des.*, 9, 297-300(2009). doi:10.1021/cg8004807

Omri, K., Najeh, I., Dhahri, R., El Ghoul, J. and El Mir, L., Effects of temperature on the optical and electrical properties of ZnO nanoparticles synthesized by sol–gel method, *Micro Elect. Engg*., 128, 53-58(2014). doi:10.1016/j.mee.2014.05.029

Prasad, R. and Rattan, G., Preparation methods and applications of CuO-CeO_2 catalysts: A short review, *Bull. Chem. React. Eng. Catal*., 5, 7-30(2010).

Radzimska, A. K. and Jesionowski, T., Zinc Oxide-From Synthesis to Application: A Review, *Materials.*, 7, 2833-2881(2014). doi:10.3390/ma7042833

Raoufi, D., Synthesis and microstructural properties of ZnO nanoparticles prepared by precipitation method, *Renewable Energy*., 50, 932-937(2013). DOI: 10.1016/j.renene.2012.08.076

Singh, J., Husdon, M. S. L., Pandy, S. K., Tiwari, R. S. and Srivatav, O. N., Structural and hydrogenation studies of ZnO and Mg doped ZnO nanowires, *Int. J. Hydrogen Energy*., 37, 3748-3754(2012). doi:10.1016/j.ijhydene.2011.04.010

Wright, G. D., Resisting resistance: new chemical strategies for battling superbugs, *Chem. Biol*., 7, R127–R132(2000). doi:10.1016/S1074-5521(00)00126-5

Xiong, H. M., Xu, Y., Ren, Q. G. and Xia, Y.Y., Stable aqueous ZnO @ polymer core-shell nanoparticles with tunable photoluminescence and their application in cell imaging, *Am. J. Chem. Soc.*, 130, 7522-7523(2008). doi:10.1021/ja800999u

Zandi, S., Kameli, P., Salamati, H., Ahmadvand, H. and Hakimi, M., Microstructure and optical properties of ZnO nanoparticles prepared by simple method, *Physica. B*., 406, 3215-3218(2011). doi:10.1016/j.physb.2011.05.026